

AD-A094 720

NAVAL SURFACE WEAPONS CENTER SILVER SPRING MD
PRODUCTION AND ASSESSMENT OF DAMAGED HIGH ENERGY PROPELLANT SAM--ETC(U)
MAY 80 W L ELBAN
NSWC/TR-79-259

F/G 21/9.2

NL

UNCLASSIFIED

1 of 1
AD-A094 720



NSWC TR 79-259

LEVEL

(12)

AD A094720

**PRODUCTION AND ASSESSMENT OF DAMAGED
HIGH ENERGY PROPELLANT SAMPLES**

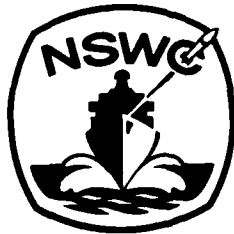
BY WAYNE L. ELBAN

RESEARCH AND TECHNOLOGY DEPARTMENT

8 MAY 1980

REC'D
FEB 9 1981
C

Approved for public release, distribution unlimited



NAVAL SURFACE WEAPONS CENTER

Dahlgren, Virginia 22448 • Silver Spring, Maryland 20910

DBG FILE COPY

81 2 09 027

UNCLASSIFIED

SECURITY CLASSIFICATION OF THIS PAGE (When Data Entered)

REPORT DOCUMENTATION PAGE		READ INSTRUCTIONS BEFORE COMPLETING FORM
1. REPORT NUMBER NSWC/TR-79-259	2. GOVT ACCESSION NO. AD A044726	3. RECIPIENT'S CATALOG NUMBER
4. TITLE (and Subtitle) Production and Assessment of Damaged High Energy Propellant Samples		5. TYPE OF REPORT & PERIOD COVERED
7. AUTHOR(s) W. L. Elban		6. PERFORMING ORG. REPORT NUMBER
9. PERFORMING ORGANIZATION NAME AND ADDRESS Naval Surface Weapons Center White Oak Silver Spring, Maryland 20910		8. CONTRACT OR GRANT NUMBER(s) SSP013
11. CONTROLLING OFFICE NAME AND ADDRESS		10. PROGRAM ELEMENT, PROJECT, TASK AREA & WORK UNIT NUMBERS 0;
14. MONITORING AGENCY NAME & ADDRESS (if different from Controlling Office)		12. REPORT DATE 8 May 1980
		13. NUMBER OF PAGES 41
		15. SECURITY CLASS. (of this report) UNCLASSIFIED
		15a. DECLASSIFICATION DOWNGRADING SCHEDULE
16. DISTRIBUTION STATEMENT (of this Report) Approved for public release; distribution unlimited.		
17. DISTRIBUTION STATEMENT (of the abstract entered in Block 20, if different from Report)		
18. SUPPLEMENTARY NOTES		
19. KEY WORDS (Continue on reverse side if necessary and identify by block number) DDT Ultrasonics Deformation Microscopy Fracture Thermal Stressing Propellant Aquarium Experiment		
20. ABSTRACT (Continue on reverse side if necessary and identify by block number) This work was undertaken to subject a variety of high energy propellants to different stress fields and to assess the microstructural changes that occur. Low strain rate mechanical deformation in compression and low temperature thermal stressing were used to damage samples. These materials were tested nondestructively using ultrasonics in which longitudinal sound velocity measurements were made. Microscopic examination was performed on microtomed		

DD FORM 1473
1 JAN 73EDITION OF 1 NOV 65 IS OBSOLETE
S/N 0102-LF-014-6601

UNCLASSIFIED

SECURITY CLASSIFICATION OF THIS PAGE (When Data Entered)

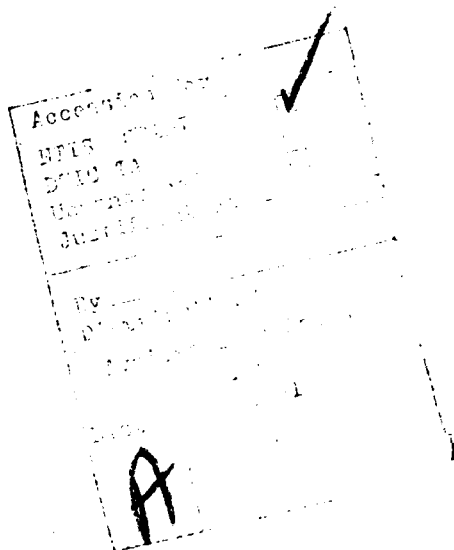
UNCLASSIFIED

SECURITY CLASSIFICATION OF THIS PAGE (When Data Entered)

20. Cont'd

sections of damaged and undamaged propellant, as well as on fracture surfaces when appropriate. Propellant recovered from a low amplitude shock sensitivity experiment, an aquarium shot, was also evaluated for comparison purposes.

In general, propellant samples that had been compressed at low strain rate did not undergo extensive damage. Crack densities were very low, and dewetting was the observed damage mechanism. Propellant samples exposed to liquid nitrogen exhibited numerous brittle fractures and little, if any, dewetting. Based on sound velocity measurements, the deformation was localized, leaving a large volume of material undisturbed. Propellant recovered from the aquarium experiment was damaged most extensively of all the material examined in this work. The crack number density and the area of crack surfaces/unit volume of propellant were highest. Sound velocity measurements indicate that dewetting did not occur in sizable portions of the material and that again the deformation was localized.




UNCLASSIFIED

SECURITY CLASSIFICATION OF THIS PAGE(When Data Entered)

FOREWORD

This work was performed for the High Energy Propellant Safety (HEPS) Program sponsored by the Strategic Systems Project Office under work request number N0003078WR82428 SSP013. The results and conclusions presented in this report concerning the production and characterization of damage in high energy propellants should be of interest to those working with the mechanical and fracture behavior of these materials. This work should also provide insight into some of the types of damage mechanisms than can occur to those investigating the influence damage has on propellant sensitivity and performance.


KURT F. MUELLER
By direction

PREFACE

R. R. Bernecker provided considerable insight into deflagration to detonation transition phenomena in high energy propellants and many suggestions that assisted in developing this work. The many helpful discussions on ultrasonic measurements with G. V. Blessing and A. L. Bertram are gratefully acknowledged. The microscopy was performed by M. K. Norr (scanning electron microscope) and R. H. Renner (light microscope). Several informative discussions were held with O. M. Dengel who demonstrated the feasibility of using exposure to liquid nitrogen to fracture high energy propellants. T. P. Liddiard provided the propellant recovered from the aquarium test and test information and characteristics. The numerous discussions with C. S. Coffey on heat generation due to deformation and fracture are recognized.

CONTENTS

	<u>Page</u>
I. INTRODUCTION.....	7
II. EXPERIMENTAL.....	9
A. PRODUCTION OF DAMAGED SAMPLES.....	9
1. MECHANICAL DEFORMATION STUDIES.....	9
2. THERMAL STRESSING EXPERIMENTS.....	9
3. RECOVERED PROPELLANT FROM AQUARIUM SHOT.....	10
B. ASSESSMENT OF DAMAGE.....	10
III. RESULTS AND DISCUSSION.....	13
A. MECHANICAL DEFORMATION STUDIES.....	13
B. THERMAL STRESSING EXPERIMENTS.....	17
C. RECOVERED PROPELLANT FROM AQUARIUM SHOT.....	23
IV. SUMMARY AND CONCLUSIONS.....	33
V. BIBLIOGRAPHY.....	35
VI. ABBREVIATIONS, ACRONYMS, AND SYMBOLS.....	37
APPENDIX A MODEL OF THE FAILURE PROCESS IN COMPOSITE SOLID PROPELLANTS.....	A-1

ILLUSTRATIONS

<u>Figure</u>		<u>Page</u>
1	Schematic Diagram of Ultrasonic Apparatus (Pulse-Echo Operation).....	11
2	Cylindrical Charges (41 mm Dia Initially) of FKM Strained in Compression to (a) -47.2%, (b) -58.5%, and (c) -69.8%.....	14
3	Longitudinal Velocity one hour after Compressing Versus Applied Engineering Compressive Strain for Propellant Samples (Nominal 40 mm Dia x 13 mm High).....	15
4	SEM Photomicrographs of Microtomed Sections of ALTU-16 (a) Strained to -9.4%, (b) Strained to -58.8%, and (c) Unstrained.....	16
5	Cylindrical Charges (38 mm Dia) of VRA-23.....	19
6	SEM Photomicrographs of Microtomed Section of Unstrained VRA-23.....	20
7	SEM Photomicrographs of Fracture Surface of VRA-23 that Resulted When Bare Charge was Immersed in Liquid Nitrogen.....	21
8	SEM Photomicrographs of Microtomed Section Approximately 1 mm Behind Primary Fracture Surface of VRA-23 that Resulted from Liquid Nitrogen Quenching.....	22
9	Largest Pieces (Initially 50 x 50 mm) of VRA-23 Recovered from Aquarium Shot.....	25
10	SEM Photomicrographs of Exposed Fracture Surface of VRA-23 Recovered from Aquarium Shot.....	28
11	SEM Photomicrographs of Microtomed Section Approximately 1 mm Behind Primary Fracture Surface of VRA-23 Recovered from Aquarium Shot.....	29
12	SEM Photomicrographs of Non-Exposed Fracture Surface of VRA-23 Recovered from Aquarium Shot.....	30

TABLES

<u>Table</u>		<u>Page</u>
1	Compilation of Results Obtained for Bare Cylindrical (38mm dia) Charges of VRA-23 Immersed in Liquid Nitrogen.....	18
2	Compilation of Results Obtained for VRA-23 Charges Subjected to Smaller Temperature Gradients.....	24
3	Compilation of Results Obtained for VRA-23 Charges Recovered from Aquarium Shot.....	26

I. INTRODUCTION

The most commonly accepted sequence of events describing how a high energy propellant rocket motor undergoes a transition from deflagration to detonation (DDT) begins with a ballistic malfunction which produces a multidimensional applied stress that heavily damages the propellant grain.¹ Obviously, since the material is consumed, little is known about the nature of the damage (generated under these stress fields) which leads to DDT. Consequently, there is a need to develop laboratory techniques or small scale experiments for generating damaged propellant samples which possess varying amounts of cracking, porosity, and/or granularity. These samples would be available for a variety of sensitivity and performance testing including determination of shock sensitivity, closed tube DDT behavior, and augmented burning rate. It is also important to use (and develop where necessary) material characterization techniques to study the nature and extent of damage that occurs.

The deformation and fracture behavior of solid propellants has been the subject of considerable experimental and theoretical work. However, ultrasonics has been used sparingly as a tool to assess damage in propellants, and little effort has been devoted to microstructural analysis either during or after stressing. In a recent study, Knollman, Martinson, and Bellin² measured changes in longitudinal velocity and attenuation of ultrasonic waves as a discrete function of strain while the material (propellant or inert) was strained either in uniaxial tension, compression, or shear. It was concluded that the changes in wave speed and attenuation were caused by dewetting. In a separate study, Dreitzler and Shih³ used ultrasonics to measure the as-manufactured porosity of propellants. A large decrease (almost 43%) in sound speed and a slight increase (about 7%) in attenuation were obtained when the porosity in the propellant increased from 0.35 to 1.35%.

¹Kincaid, J. F., "The Inadvertent Detonation of Large Solid Motors Loaded with High Energy Propellants," in ONR/AFOSR Workshop on Deflagration-to-Detonation Transition, CPIA Publ. 299, 11-13 Jan 1978; publ 1978, pp. 5-18.

²Knollman, G. C., Martinson, R. H., and Bellin, J. L., "Ultrasonic Assessment of Cumulative Internal Damage in Filled Polymers," Journal of Applied Physics, Vol. 50, No. 1, 1979, pp. 111-120.

³Dreitzler, D. R. and Shih, C. C., "Porosity Measurement of Solid Propellants Using Ultrasonic Techniques," in Proceedings of the 1978 JANNAF Propulsion Meeting, Vol. I, CPIA Publ. 293, 14-16 Feb 1978; publ 1978, pp. 115-125.

The scanning electron microscope (SEM) has been used by Cornwell and Schapery⁴ to observe in situ straining of solid propellant. A series of photomicrographs showing the material under increasing tensile strain was obtained; it was observed that cracks grow at or in the vicinity of the filler particle-polymer matrix interface. Large cavities around the filler particles were observed and appeared circular just prior to failure. No evidence was obtained for fracture occurring in filler particles.

The dynamic fracture and fragmentation behavior of high energy propellant at high strain rates has been investigated by Murri, Horie, and Curran⁵ using a plate slap technique. From photomicrographs of the damaged propellant, it was hypothesized that HMX crystals are weakly bonded to the matrix and serve to nucleate cracks under applied tensile stresses. When the dynamic tensile stresses are sufficiently high, these cracks then grow and coalesce to form fragments. Microscopic examination of recovered fragments revealed that cracks were present and that debonding between the HMX and the propellant matrix had occurred. There was also evidence of fracture of HMX crystals.

This work was undertaken to subject a variety of high energy propellants to different stress fields and to assess the microstructural changes that occur. Low strain rate mechanical deformation in compression and low temperature thermal stressing were used to damage samples. These materials were tested nondestructively using ultrasonics in which longitudinal sound velocity measurements were made. Microscopic examination was performed on microtomed sections of damaged and undamaged propellant, as well as on fracture surfaces when appropriate. Propellant recovered from a low amplitude shock sensitivity experiment, an aquarium shot, was also evaluated for comparison purposes.

⁴Cornwell, L. R. and Schapery, R. A., "SEM Study of the Microcracking in Strained Solid Propellant," Metallography, Vol. 8, No. 5, 1975, pp. 445-452.

⁵Murri, W. J., Horie, Y., and Curran, D. R., "Fracture and Fragmentation of High Energy Propellant," SRI International Annual Report, Mar 1978.

II. EXPERIMENTAL

A. PRODUCTION OF DAMAGED SAMPLES

1. MECHANICAL DEFORMATION STUDIES. Four propellant formulations were utilized in this investigation. These were FKM (a modified double-base propellant), VOY-4 and VMX-2J, (modified double-base high energy propellants), and ALTU-16 (an experimental high energy composite propellant). All of these compositions contain ammonium perchlorate and HMX as crystalline oxidizers and aluminum as a fuel. A number of approximately 40 mm diameter, 13 mm high cylinders were machined from blocks of these materials. The machined surfaces were smooth, and the ends were parallel to each other to within 0.02 mm.

All samples were strained remotely in compression using a hydraulic press operating at a strain rate of approximately 0.2 s^{-1} . Engineering strains,

$$e = \frac{l - l_0}{l_0}, \text{ ranging from approximately } -10 \text{ to } -60\% \text{ were achieved by pressing}$$

to heights set by gage blocks for a dwell time of 120 s. Disks of 0.3 mm Teflon sheet were inserted between the sample and press platens to reduce friction in an effort to retain uniaxial strain at the higher strain levels and also as a safety precaution. Following the 120 s dwell time, the stress was completely released, and the samples were allowed to relax.

2. THERMAL STRESSING EXPERIMENTS. Only one propellant formulation, VRA-23, a modified double-base high energy propellant, was studied. This composition also contains ammonium perchlorate, HMX, and aluminum. Several approximately 38 mm diameter cylinders of varying heights (roughly ranging from 8 to 12 mm) were immersed in liquid nitrogen, as bare charges, for varying lengths of time up to 0.5 h. In addition, a series of experiments were performed in which samples, cut from 13 mm thick slab material, were exposed to less severe thermal gradients. Two approaches were pursued. First, one sample was placed in a Webber cold box (approximate temperature = -52°C) for 0.5, 1, and 96 h. At the end of each exposure time interval, the sample was removed from the cold box, allowed to warm up to room temperature, and examined. The second approach involved surrounding the propellant with thermal insulation. Vermiculite was chosen as the insulating material. A new VRA-23 sample was placed in a small cardboard box surrounded by 3-4 mm of vermiculite (~ 1-2 mm granules), and the box was immersed in liquid nitrogen for 2 h. On removal, it was found that liquid nitrogen had permeated the box and was in contact with the sample. Again, the sample was allowed to warm up to room temperature and examined.

3. RECOVERED PROPELLANT FROM AQUARIUM SHOT. Some VRA-23 propellant that was recovered from an aquarium shot was examined many days after being shocked. The aquarium experiment is a shock sensitivity test⁶ for determining the threshold of burning and/or detonation for low amplitude-long duration shock waves. The configuration of the propellant sample had been two 50 X 50 X 13 mm thick slabs taped back to back which experienced a shock having an input pressure of approximately 1.25 GPa and a pulse duration of 25-30 μ s.

B. ASSESSMENT OF DAMAGE

Damage in propellant samples subjected to the various stress fields described previously was evaluated using ultrasonics and microscopy as well as visual observation. Residual strain values were calculated from axial dimensional measurements made before and after stressing.

A schematic of the ultrasonic apparatus used for making the axial longitudinal sound velocity measurements appears in Figure 1. The basic component is a broadband ultrasonic pulser/receiver (Panametrics Model 5055 PR) which is combined with two 25 mm diameter broadband contact transducers (Panametrics V102) having a center frequency of 1 MHz. Since the operation^{7,8} of this instrumentation has been described in detail elsewhere, very little description will be given. This system can be operated in two different modes: pulse-echo and through-transmission. In pulse-echo, ultrasonic pulses are received by the transmitting transducer after being reflected off the backwall, while in through-transmission, a separate receiving transducer is positioned at the backwall. The latter mode of operation was employed when the strained samples were too highly attenuating to permit pulse-echo operation. A viscous couplant, such as honey or silicone stopcock grease, is used to transmit the ultrasonic energy between the transducer and the test specimen. Signal amplitude versus time output is displayed on an oscilloscope (Tektronix Model 545B), and transit time measurements (horizontal axis) are made directly from the cathode ray tube screen. It is estimated that the velocities obtained for the system operating in pulse-echo are accurate to about 1%, while through-transmission errors may be as high as 5%.

The SEM was used extensively to examine microtomed* sections of stressed propellant samples. These were compared to microtomed surfaces of unstressed material in an effort to identify the various damage mechanisms that were operating.

⁶ Liddiard, T. P., "The Initiation of Burning in High Explosives by Shock Waves," in Proceedings of the Fourth Symposium on Detonation, Publ. ACR-126, 12-15 Oct 1965; publ 1966, pp. 487-495.

⁷ Krautkramer, J. and Krautkramer, H., Ultrasonic Testing of Materials (New York: Springer-Verlag, 1969), pp. 151-196.

⁸ Pollard, H. F., Sound Waves in Solids (London: Pion Ltd., 1977), pp. 157-159.

*Some sectioning was performed using a single-edge razor instead of a microtome. No difference in appearance could be detected in viewing surfaces of unstressed material obtained with these two cutting tools. Consequently, sectioned propellant will always be referred to as "microtomed".

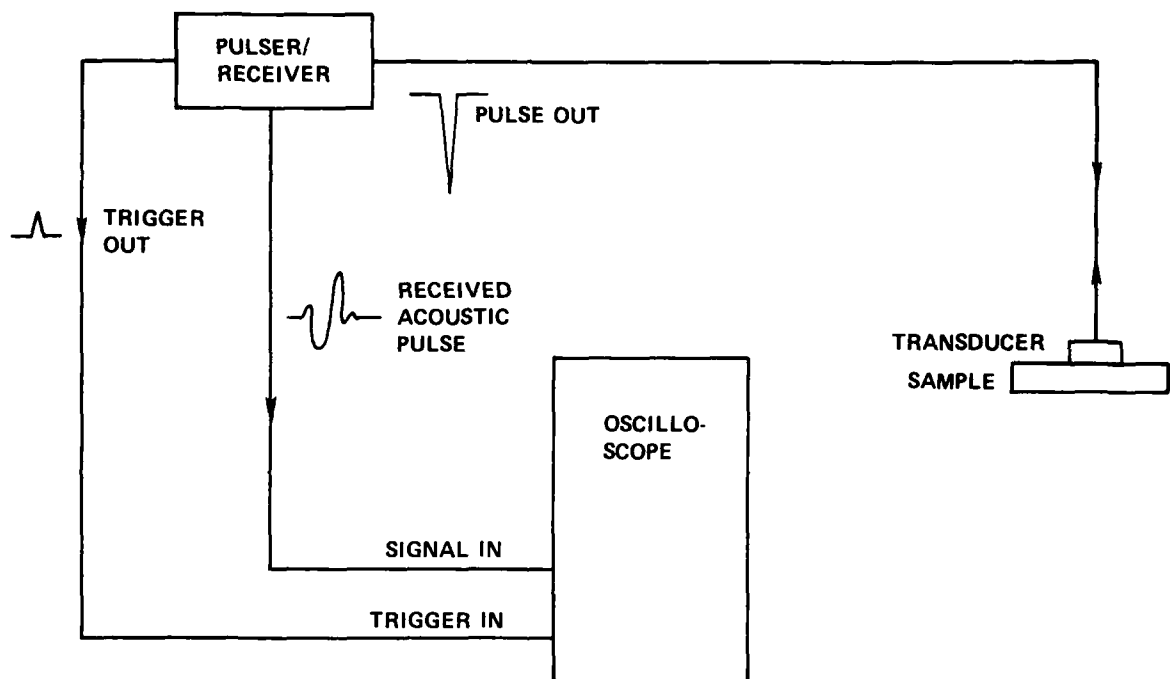


FIGURE 1 SCHEMATIC DIAGRAM OF ULTRASONIC APPARATUS
(PULSE-ECHO OPERATION)
(TAKEN FROM REFERENCE 11).

In addition, many of the fracture surfaces that resulted were examined using the SEM. The operation and use of the SEM⁹ has been discussed in detail and will not be reviewed in this work. Sample preparation is worth mentioning, however. All of the propellant specimens that were examined were non-conductive and required the application of a thin conducting coating. This was accomplished by vacuum depositing first a carbon layer, followed by a layer of a gold-palladium alloy. In an effort to minimize electron beam damage, samples were viewed at low magnification (25-50X) first, and then the magnification was increased to 1000X maximum. There was no evidence of beam damage in any of the samples at these magnifications during the exposure periods.

Some of the microtomed specimens were also examined using the light microscope operating at low magnification (about 73X). Although optical microscopy is an exceedingly valuable technique for investigating structures of materials,¹⁰ it does have a serious deficiency that hinders its application in this work. Usually, the depth of field is limited sufficiently to prohibit viewing the entire specimen in focus, even though microtoming provides a reasonably flat surface. Although some worthwhile photomicrographs were obtained with the light microscope, those chosen for discussion purposes were obtained using the SEM.

⁹ Hearle, J. W. S., Sparrow, J. T., and Cross, P. M., The Use of the Scanning Electron Microscope (Oxford: Pergamon Press, 1972).

¹⁰ Richardson, J. H., Optical Microscopy for the Materials Sciences (New York: Marcel Dekker, Inc., 1971).

III. RESULTS AND DISCUSSION

A. MECHANICAL DEFORMATION STUDIES

The results¹¹ for straining FKM, VOY-4, VMX-2J, and ALTU-16 in compression have been reported previously, and only a summary will be given, including some of the more interesting results. In general, the samples that had been mechanically deformed at the low strain rate used in this work did not exhibit extensive damage. Crack densities were found to be very low. The propellant exhibiting the most visible damage was FKM, and the cylinders subjected to the three highest strains appear in Figure 2. For this particular material, there were numerous cracks (see samples strained to -58.5 and -69.8%) at the casting grain boundaries. Very little cracking was visible in the cylinders of the remaining compositions. Longitudinal velocity measurements¹¹ one hour after compressing to various strain levels are given in Figure 3 for the various propellants. In each instance, there was a decrease in sound speed with increasing applied strain, although the rate of decrease differed markedly. Reductions in sound speed, by as much as 88%, were obtained for ALTU-16.

Microscopic examination of microtomed cross-sections of stressed propellant did not reveal gross cracking in the propellant (except for FKM) or cracking in ingredient particles to be widespread damage mechanisms. It is considered unlikely that these make a significant contribution to the change in longitudinal velocity as a function of compressive strain. The damage mechanism that was observed is dewetting¹² or failure of the interfacial bond between filler particles and the polymer matrix. As an example, a set of SEM photomicrographs¹¹ that were obtained for sections of ALTU-16 is given Figure 4. Each sample exhibited numerous debonded crystals, but no incident cracks were observed. There was some evidence of cracked crystals that is attributed to the microtoming operation. Although it is difficult to distinguish between the extent of damage for the surfaces of samples strained to various levels, the sample strained to -58.8% did display the most debonding. It was concluded that vacuole formation (see Appendix A) is responsible (either partially or totally) for the decrease in longitudinal velocity with increasing strain.¹¹ It was not determined

¹¹ Elban, W. L., Bertram, A. L., Blessing, G. V., and Bernecker, R. R., "The Use of Ultrasonics for the Nondestructive Evaluation of Damage in Mechanically Deformed Propellants," Unclassified; unlimited report within Proceedings of the 15th JANNAF Combustion Meeting, Vol. III, CPIA Publ. 297, 11-15 Sep 1978; publ 1979 (CONFIDENTIAL), pp. 49-73.

¹² Oberth, A. E., "Principle of Strength Reinforcement in Filler Rubbers," Rubber Chemistry and Technology, Vol. 40, No. 5, 1967, pp. 1337-1363.

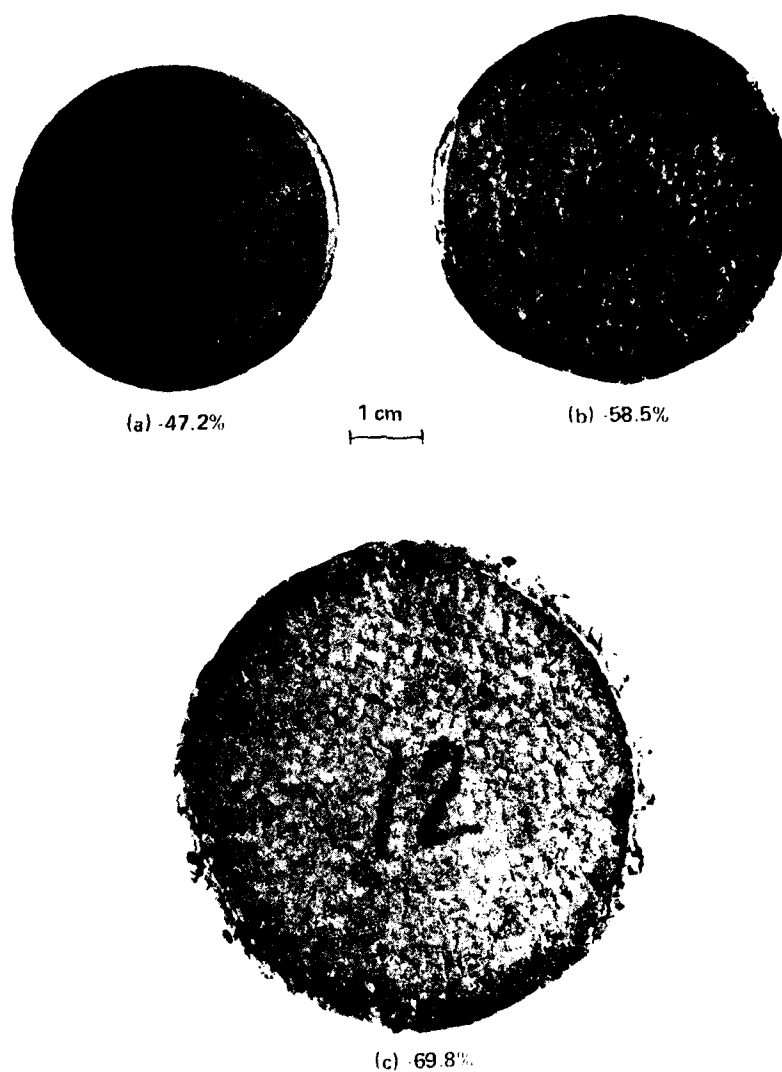


FIGURE 2 CYLINDRICAL CHARGES (41 mm DIA INITIALLY) OF FKX STRAINED IN COMPRESSION TO (a) -47.2%, (b) -58.5%, AND (c) -69.8%

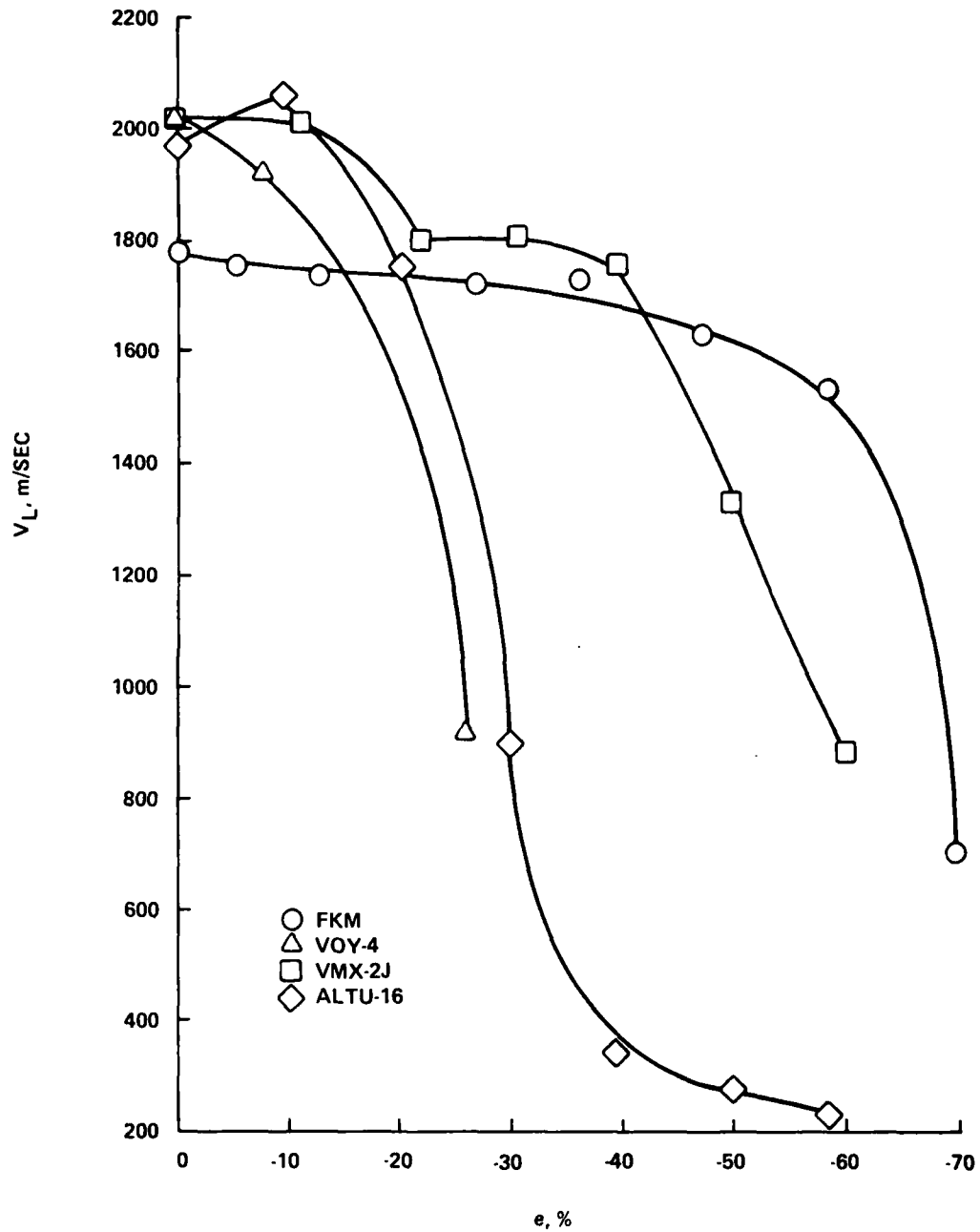
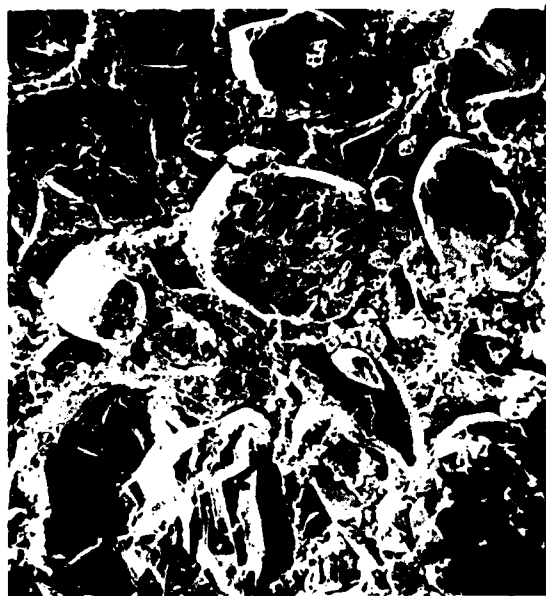
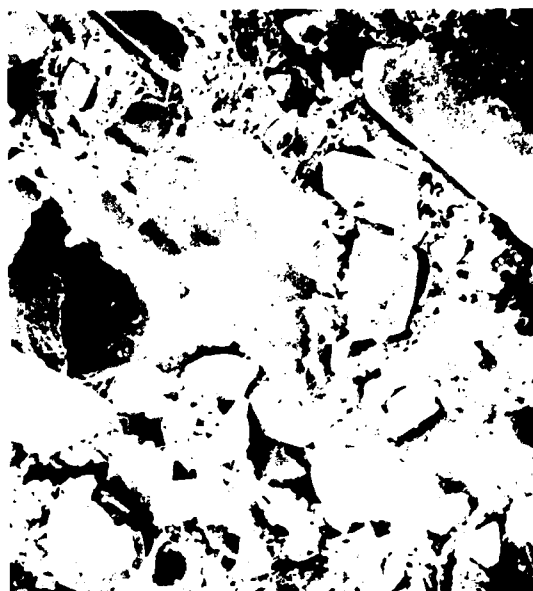


FIGURE 3 LONGITUDINAL VELOCITY ONE HOUR AFTER COMPRESSING VERSUS APPLIED ENGINEERING COMPRESSIVE STRAIN FOR PROPELLANT SAMPLES (NOMINAL 40 mm DIA x 13 mm HIGH) (TAKEN FROM REFERENCE II).



(a) -9.4%



(b) -58.8%

100 μ m
└───┘



(c) UNSTRAINED

FIGURE 4 SEM PHOTOMICROGRAPHS OF MICROTOMED SECTIONS OF ALTU-16 (a) STRAINED TO -9.4%, (b) STRAINED TO -58.8%, AND (c) UNSTRAINED (TAKEN FROM REFERENCE II).

whether non-visible damage, such as deformation in the propellant binder or dislocation generation in the filler crystals, also makes a significant contribution.

B. THERMAL STRESSING EXPERIMENTS

The results obtained for bare cylindrical charges (38 mm diameter) of VRA-23 immersed in liquid nitrogen for various lengths of time are given in Table 1. Each of the samples cracked into a number of pieces (see bottom two cylinders in Figure 5), and numerous small cracks were visible in each of the pieces. Visual inspection of the fracture surfaces revealed that the material underwent brittle fracture. The length of each sample was measured at room temperature before and after quenching, and no dimensional change was detected within the accuracy of the measurement. Only a slight decrease in longitudinal velocity was obtained for a sample immersed in liquid nitrogen for thirty minutes and allowed to warm to room temperature.

A number of interesting observations can be made from the SEM photomicrographs taken of material that had been immersed in liquid nitrogen. For comparison purposes, a microtomed cross-section of undamaged VRA-23 appears in Figure 6. The surface that results is monolithic in appearance with the largest exposed crystals (probably HMX) being about 200 μm . In a few instances, it appears that the cutting operation has caused debonding to occur at the binder-crystal interface. The fracture surface that results when a bare cylindrical charge of VRA-23 is immersed in liquid nitrogen is shown in Figure 7. Although this surface reveals more topographical detail than the microtomed surface, it is still fairly flat and featureless. Additional cracks do not intersect this primary fracture surface, and there is little indication that dewetting has occurred. However, numerous pores having characteristic dimensions ranging from 5 to 15 μm can be observed. The origin of these pores is not definitely known, but it is felt some water soluble ingredient (probably ammonium perchlorate) has been leached from the surface while the sample warmed to room temperature. It was observed that almost immediately after removal from liquid nitrogen, the sample fragments became covered by ice which eventually melted and ran off.

A microtomed cross-section approximately 1 mm behind the primary fracture surface generated during immersion in liquid nitrogen is displayed in Figure 8. Several cracks that did not extend to an exterior surface are visible. These cracks are straight and have smooth surfaces, exhibiting a largely brittle character. The porosity noted in the fracture surface displayed in Figure 7 was not observed in this cross-section, indicating that this porosity is a surface phenomena that does not occur in the bulk material. Perhaps the most interesting feature in Figure 8 (see bottom portion of lower magnification photomicrograph) is the crystal (believed to be HMX) that was fractured as a crack propagated through the propellant. Clearly, for these sample loading conditions, the binder-particle interfacial bond exceeded the tensile fracture stress of the HMX crystal. Evidence for fracture of HMX crystals was also obtained from examining recovered VRA-23 propellant that had experienced high strain rate impact by a flyer plate.⁵ However, the propellant fracture surfaces that resulted in these experiments do not reveal nearly as much brittle character as those obtained in the present work. It is concluded that the fracture obtained by bare charge immersion in liquid nitrogen was too severe to be useful in subsequent DDT experiments or comparison sensitivity tests.

⁵ See footnote 5 on page 8.

TABLE 1 COMPILATION OF RESULTS OBTAINED FOR BARE CYLINDRICAL
(38MM DIA) CHARGES OF VRA-23 IMMersed IN LIQUID NITROGEN

Initial Sample Length (mm)	Final Sample Length (mm)	Immersion Time	Audible Cracking Noise	Fracture	V_L^* (m/s)
11.65- 11.68	11.62- 11.68	30 min	< 1 min	Many Pieces; Brittle	1850
9.70- 9.72	9.68- 9.70	~36 s	~35 s	Many Pieces; Brittle	Not Determined
8.28- 8.30	8.25- 8.28	~21 s	~20 s	Many Pieces; Brittle	Not Determined

*Pulse-echo; $f_c = 1$ MHz; V_L for undamaged VRA-23 is 1880 m/s.

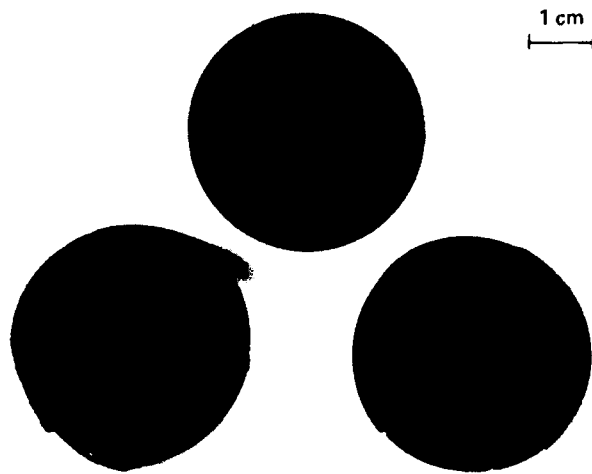


FIGURE 5 CYLINDRICAL CHARGES (38 mm DIA) OF VRA-23
TOP: CONTROL, HAS NOT BEEN THERMALLY
STRESSED. BOTTOM: PIECES RECOVERED FROM
BARE CHARGES IMMERSSED IN LIQUID NITROGEN.

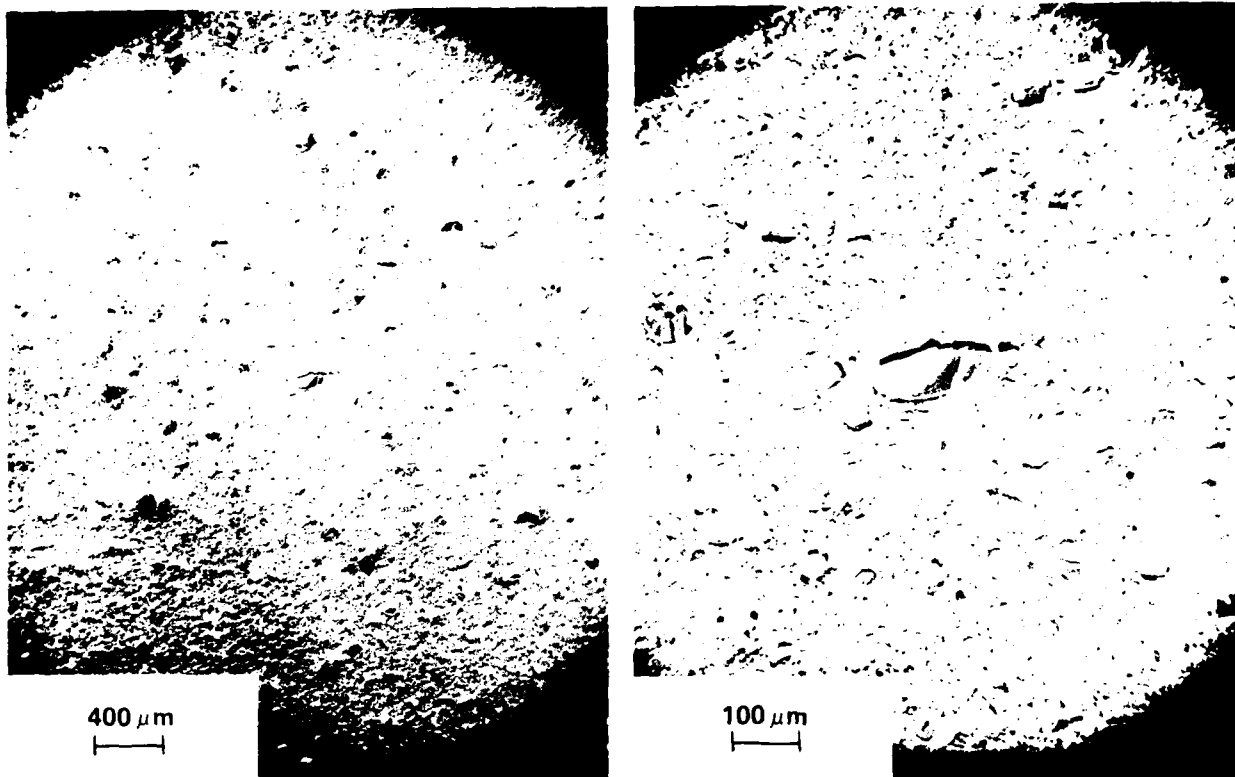


FIGURE 6 SEM PHOTOMICROGRAPHS OF MICROTOMED SECTION OF UNSTRAINED VRA-23

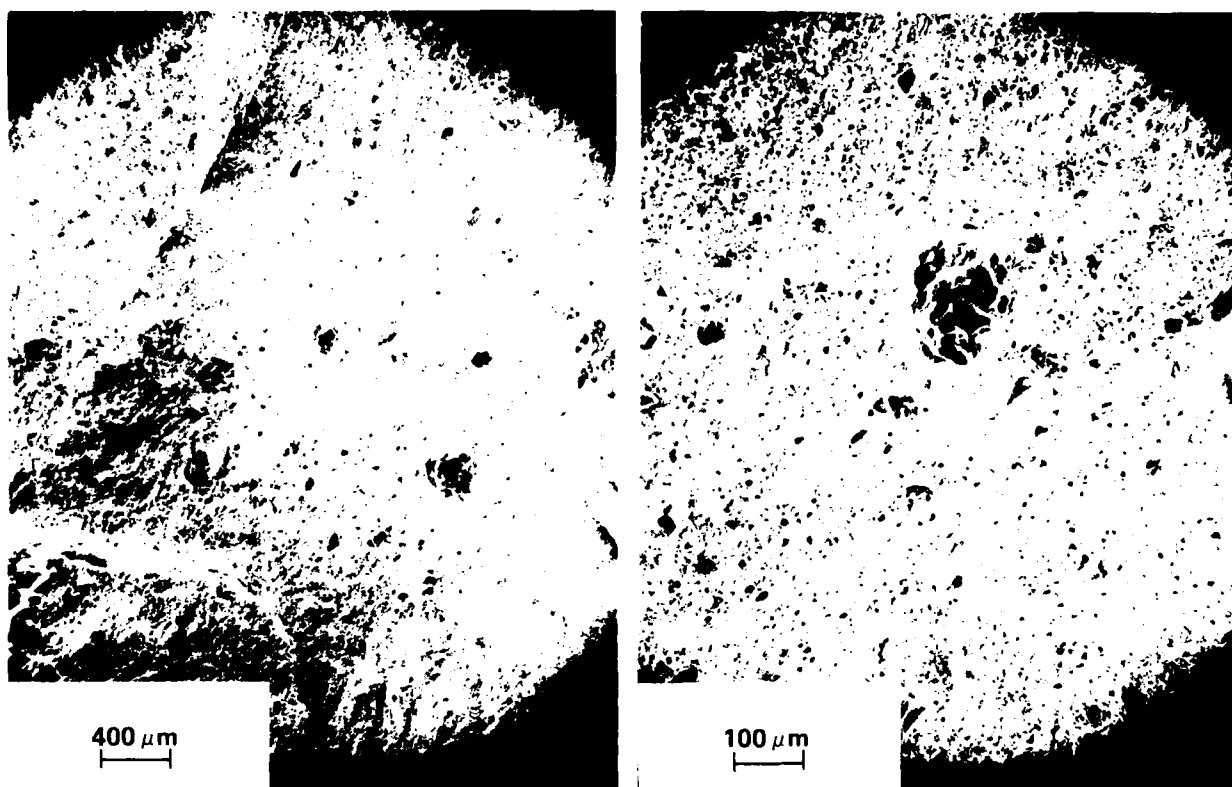


FIGURE 7 SEM PHOTOMICROGRAPHS OF FRACTURE SURFACE OF VRA-23 THAT
RESULTED WHEN BARE CHARGE WAS IMMERSSED IN LIQUID NITROGEN

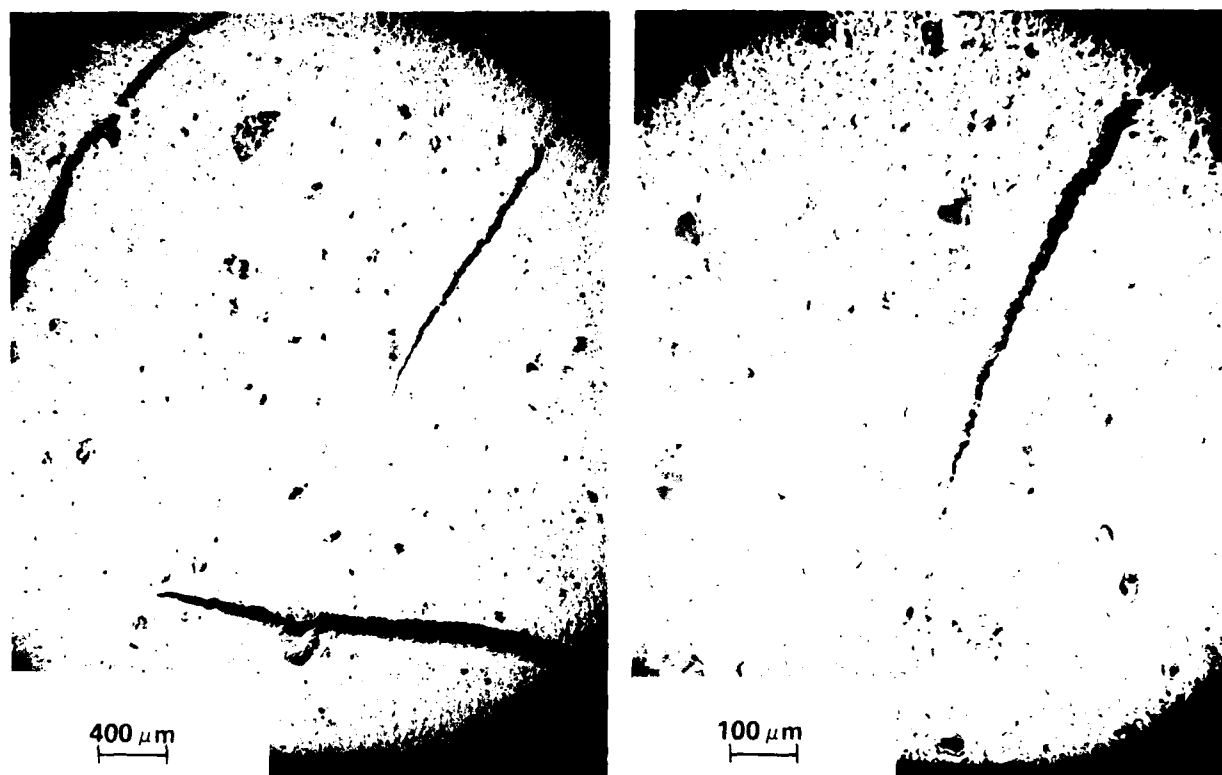


FIGURE 8 SEM PHOTOMICROGRAPHS OF MICROTOMED SECTION APPROXIMATELY 1 mm BEHIND PRIMARY FRACTURE SURFACE OF VRA-23 THAT RESULTED FROM LIQUID NITROGEN QUENCHING

In an attempt to lessen the severity of the cracking, a series of experiments were performed in which samples of VRA-23 (taken from 13 mm thick slab material) were exposed to smaller thermal gradients. These results are compiled in Table 2. Virtually no change in longitudinal velocity was obtained for either the sample exposed to -52°C for 96 h or the sample insulated with vermiculite and immersed in liquid nitrogen. It is concluded that these smaller temperature gradient experiments were not successful in providing material having high crack densities (in fact, no cracks were observed). Although it should be possible to develop a controlled thermal stressing technique for obtaining samples having large densities of smaller length cracks, the nature of brittle fracture is such to make this a very difficult task. According to the Griffith energy-balance concept¹³ for characterizing crack propagation in purely brittle solids, if the applied stress exceeds a critical level, the crack will propagate spontaneously without limit. Thus, it is unlikely that during thermal stressing, cracks will propagate in brittle materials without many extending to exterior surfaces, leaving the material in a fragmented state.

In comparing the results from the thermal stressing experiments with the findings from the mechanical deformation studies, it is clear that the crack number density and the area of crack surface/unit volume of propellant increased significantly for the material exposed to liquid nitrogen. The low temperature brittle fracture indicates a significant reduction in ultimate elongation and points to the temperature dependency of the mechanical properties of VRA-23. This is expected since the stress-strain behavior of materials is temperature and strain rate dependent and since strong strain rate sensitivity for VRA-23 has been demonstrated from split Hopkinson bar experiments.⁵ The constancy of the sound speed measurements (see Table 1) suggests that very little dewetting occurred in the samples that were exposed to liquid nitrogen. Confirmed by microscopic examination, this indicates that the deformation leading to fracture is highly localized, leaving much of the material virtually undeformed.

C. RECOVERED PROPELLANT FROM AQUARIUM SHOT

The VRA-23 propellant recovered from the aquarium experiment was heavily fragmented into granules and pieces of various sizes. The two largest pieces appear in Figure 9. Visual inspection of this material revealed that extensive cracking had occurred. The cracks exhibited considerable tortuosity and were unlike the straight faceted cracks associated with thermal stressing, as seen in Figure 5. The exposed fracture surfaces were rough indicating that the cracking was non-brittle. Residual strain and longitudinal sound velocity measurements (in the thickness dimension) were made on perimeter and center regions of the larger recovered piece. These results are listed in Table 3. Each region had a small compressive residual strain, while the longitudinal velocity was found to increase slightly. An increase in longitudinal sound velocity was observed similarly (see Figure 3) for VMX-2J and ALTU-16 having small compressive residual strains obtained by mechanical stressing.¹¹ It is important

¹³Lawn, B. R. and Wilshaw, T. R., Fracture of Brittle Solids (Cambridge: Cambridge University Press, 1975), pp. 5-9.

⁵See footnote 5 on page 8.

¹¹See footnote 11 on page 13.

TABLE 2 COMPILATION OF RESULTS OBTAINED FOR VRA-23 CHARGES
SUBJECTED TO SMALLER TEMPERATURE GRADIENTS

Temperature (°C)	Exposure Time (h)	V_L^* (m/s)	Observations
-51	0.5	Not Determined	No Cracking
-52	1	Not Determined	No Cracking
-52	96	1890	No Cracking
<hr/>			
Liquid Nitrogen **	2	1870	No Cracking

*Pulse-echo; $f_c = 1$ MHz; V_L for undamaged VRA-23 is 1880 m/s.

**Sample insulated with about 3-4 mm of vermiculite.



FIGURE 9 LARGEST PIECES (INITIALLY 50 x 50 mm) OF VRA-23
RECOVERED FROM AQUARIUM SHOT

TABLE 3 COMPILATION OF RESULTS OBTAINED FOR VRA-23 CHARGES
RECOVERED FROM AQUARIUM SHOT

Sample Location	Residual Strain (%)	V_L^* (m/s)	Observations
Perimeter	-1.2	1940	Extensive Cracking; Non-Brittle
Center	-0.6	1910	Extensive Cracking; Non-Brittle

*Through-transmission; $f_c = 1$ MHz; V_L for undamaged VRA-23 is 1880 m/s.

to note that the residual strain and longitudinal velocity did not change significantly for material that had undergone considerable cracking.

Some SEM photomicrographs were obtained, allowing several additional interesting observations. An exposed fracture surface is displayed in Figure 10. Considerable roughness is evident along with numerous secondary cracks intersecting the primary fracture surface. Interfacial bond failures are visible in a few instances, although there is a lack of discernible filler particles. Light gray secondary phase particles are also conspicuous, particularly in the higher magnification photomicrograph. The origin of these particles is not known. They may be reaction products from an early stage burning reaction (see SEM photomicrographs of burned propellant surfaces that were extinguished obtained by Derr and Boggs)¹⁴ or corrosion products resulting from the fractured material being exposed to the aqueous environment. Additional attempts to locate secondary phase particles on exposed fracture surfaces from other regions of the samples were unsuccessful.

A microtomed cross-section approximately 1 mm behind the primary fracture surface appears in Figure 11. The tortuous character of the cracks is quite visible, but no secondary phase particles could be found. Further, there was no other indication that a burning reaction had occurred in or near the cracked regions. The fracture surface of a non-exposed "zero-width" crack is shown in Figure 12. This surface closely resembled the one appearing in Figure 10, except for the absence of secondary phase particles. Thus, it appears that the presence of the secondary phase particles is highly localized. In addition, no fractured HMX crystals were observed in any of the photomicrographs taken of propellant recovered from the aquarium test.

Of all of the samples examined in this work, the damage was most extensive in the propellant recovered from the aquarium shot. The small compressive residual strain and the slight increase in longitudinal velocity suggest that the samples experienced a small applied compressive stress and that dewetting did not occur. Apparently, there was increased intimacy at the binder-filler interface, and yet considerable tearing and rupture occurred. This is difficult to resolve considering the sequence of events leading to failure in composite solid propellants given in Appendix A. The most likely explanation lies in the fact that, for the aquarium experiment, the deformation occurs at high strain rate (estimated to be greater than 10^4 s^{-1}). In addition, the strain rate sensitivity of the material is probably such that the elongation at break is very low for the loading conditions of this experiment. Thus, the possibility for dewetting to occur is virtually eliminated. Analogous to propellant exposed to liquid nitrogen, the deformation leading to fracture in propellant recovered from the aquarium shot must be localized also, leaving sizable portions of relatively undisturbed material for the sound velocity measurements that were obtained. The failure pattern observed in Figure 9 is not consistent with any of the conventional compression failure modes¹⁵:

¹⁴Derr, R. L. and Boggs, T. L., "Role of Scanning Electron Microscopy in the Study of Solid Propellant Combustion: Part III The Surface Structure and Profile Characteristics of Burning Composite Solid Propellants," Combustion Science and Technology, Vol. 1, No. 5, 1970, pp. 369-384.

¹⁵Kendall, K., "Complexities of Compression Failure," Proceedings of the Royal Society of London, Ser. A, Vol. 361, No. 1705, 1978, pp. 245-263.

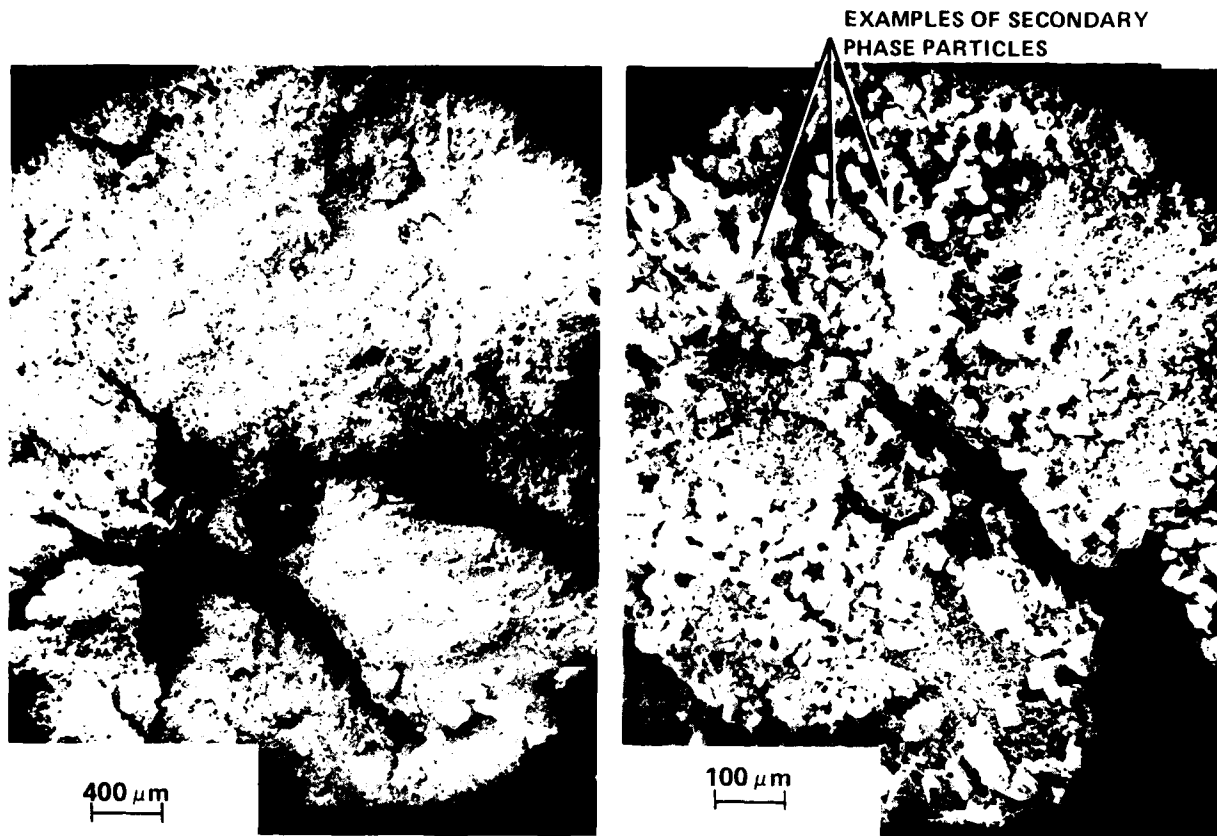


FIGURE 10 SEM PHOTOMICROGRAPHS OF EXPOSED FRACTURE SURFACE OF VRA-23
RECOVERED FROM AQUARIUM SHOT

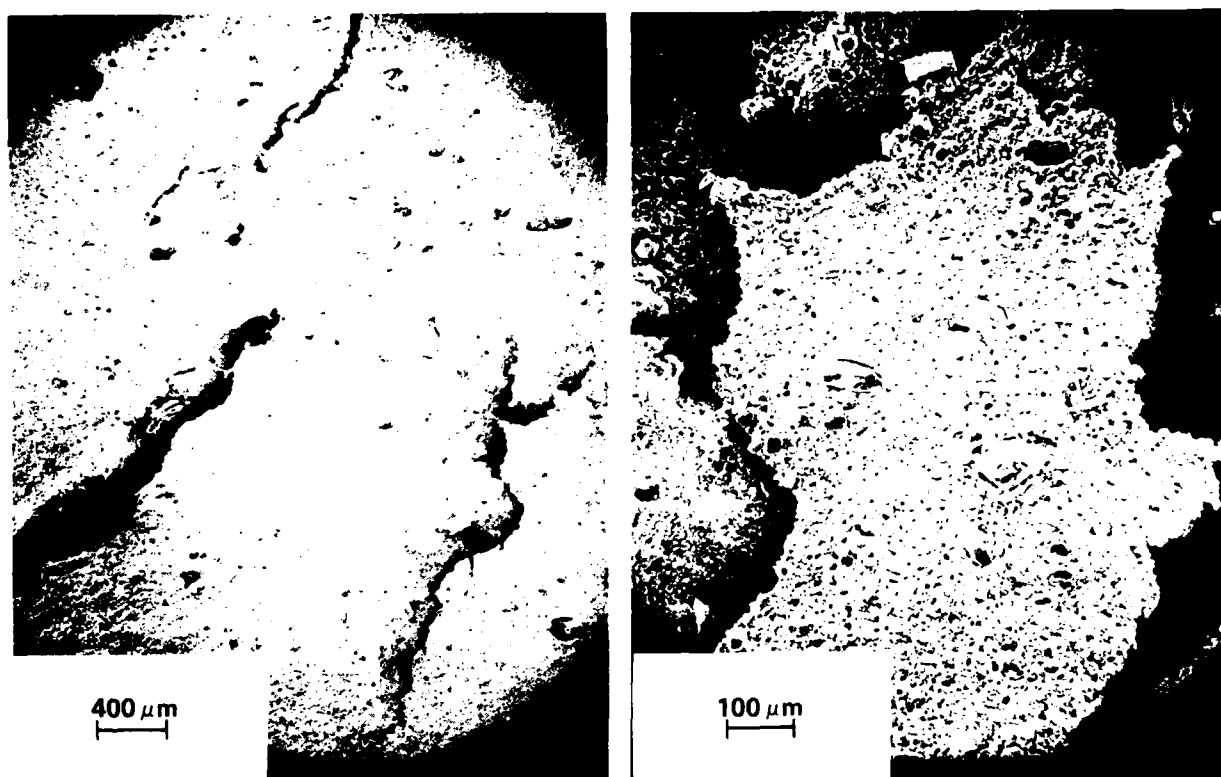


FIGURE 11 SEM PHOTOMICROGRAPHS OF MICROTOMED SECTION APPROXIMATELY 1 mm BEHIND PRIMARY FRACTURE SURFACE OF VRA-23 RECOVERED FROM AQUARIUM SHOT

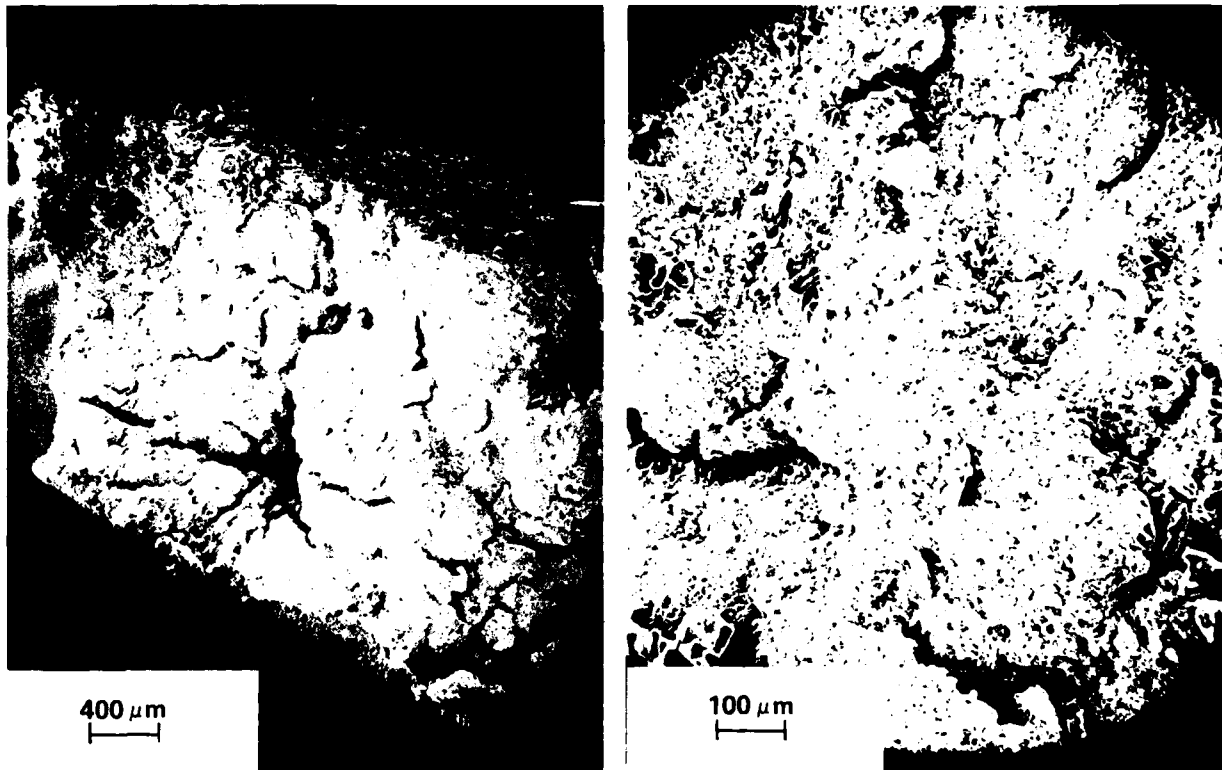


FIGURE 12 SEM PHOTOMICROGRAPHS OF NON-EXPOSED FRACTURE SURFACE OF VRA-23
RECOVERED FROM AQUARIUM SHOT

plastic yielding, cone failure, and axial splitting. The reason for this is not readily understood. Fracture caused by out-gassing of reaction products from an early stage shock-induced burning reaction in the bulk propellant is one possible explanation. Damage associated with postshock impact may have occurred also.

The extensive damage found in propellant recovered from the aquarium experiment serves to emphasize the attractiveness of developing an inexpensive variation of the aquarium test that would use a low amplitude-long duration shock to damage propellant for subsequent sensitivity and performance testing. However, this does not involve an in situ arrangement where damage and testing occur simultaneously (or follow very closely in sequence). This is an important consideration since there is increasing evidence that considerable localized heating occurs when materials undergo deformation and fracture, especially at high strain rates ($\geq 10^3 \text{ s}^{-1}$). Winter and Field¹⁶ investigated the impact initiation of explosives by striking single crystal targets (explosive) with tiny spherical particles (inert). Initiation resulted when critical conditions for particle size and velocity were exceeded. A nice feature of this experiment is the ability to examine and characterize the deformation that resulted when the impact conditions were slightly below the critical conditions necessary for initiation. Typically, the impact sites were smooth plastic indentations and few fractures were found. It was observed further that the deformation was highly localized in narrow bands of material, which were proposed to form by adiabatic shear. Although it was suggested that the mechanism responsible for initiation is the production of high local temperatures as a result of the adiabatic shear deformation, no temperature measurements were attempted.

However, in somewhat related work the temperature rise at the tip of a fast-moving crack has been found to be quite high for several different types of materials. Fuller, Fox, and Field¹⁷ used thermocouples, a temperature sensitive liquid crystal, and an infrared detector to obtain temperature rises of about 400 and 500°K for polystyrene and polymethylmethacrylate, respectively. The temperature at the tip of cracks in glass and quartz was measured by Weichert and Schönert¹⁸ using a four wavelength radiation thermometer and interpreting the observed light emission as thermal radiation. Values of 3200 and 4700°K were obtained for glass and quartz respectively. Thus, it is clear that the high energy density in the vicinity of a fast moving crack causes irreversible deformation which is dissipated as heat. There is a need to develop laboratory experiments to determine the contribution this heat production has on the DDT susceptibility of high energy propellants.

¹⁶ Winter, R. E. and Field, J. E., "The Role of Localized Plastic Flow in the Impact Initiation of Explosives," Proceedings of the Royal Society of London, Ser. A, Vol. 343, No. 1634, 1975, pp. 399-413.

¹⁷ Fuller, K. N. G., Fox, P. G., and Field, J. E., "The Temperature Rise at the Tip of Fast-Moving Cracks in Glassy Polymers," Proceedings of the Royal Society of London, Ser. A, Vol. 341, No. 1627, 1975, pp. 537-557.

¹⁸ Weichert, R. and Schönert, K., "Heat Generation at the Tip of a Moving Crack," Journal of the Mechanics and Physics of Solids, Vol. 26, No. 3, 1978, pp. 151-161.

IV. SUMMARY AND CONCLUSIONS

A. In general, propellant samples that had been compressed at low strain rate did not undergo extensive damage. Crack densities were very low, and dewetting was the observed damage mechanism.

B. Propellant samples exposed to liquid nitrogen exhibited numerous brittle fractures and little, if any, dewetting. Based on sound velocity measurements, the deformation was localized, leaving a large volume of material undisturbed. The low temperature brittleness indicates a substantial reduction in ultimate elongation.

C. Propellant recovered from the aquarium experiment was damaged most extensively of all the material examined in this work. The crack number density and the area of crack surfaces/unit volume of propellant were highest. Although the recovered material was heavily fragmented into granules and pieces of various size, sound velocity measurements indicate that dewetting did not occur in sizable portions of the material and that the deformation was localized.

V. BIBLIOGRAPHY

Cornwell, L. R. and Schapery, R. A., "SEM Study of the Microcracking in Strained Solid Propellant, "Metallography, Vol. 8, No. 5, 1975, pp. 445-452.

Derr, R. L. and Boggs, T. L., "Role of Scanning Electron Microscopy in the Study of Solid Propellant Combustion: Part III The Surface Structure and Profile Characteristics of Burning Composite Solid Propellants," Combustion Science and Technology, Vol. 1, No. 5, 1970, pp. 369-384.

Dreitzler, D. R. and Shih, C. C., "Porosity Measurement of Solid Propellants Using Ultrasonic Techniques," in Proceedings of the 1978 JANNAF Propulsion Meeting, Vol. I, CPIA Publ. 293, 14-16 Feb 1978; publ 1978, pp. 115-125.

Elban, W. L., Bertram, A. L., Blessing, G. V., and Bernecker, R. R., "The Use of Ultrasonics for the Nondestructive Evaluation of Damage in Mechanically Deformed Propellants," Unclassified; unlimited report within Proceedings of the 15th JANNAF Combustion Meeting, Vol. III, CPIA Publ. 297, 11-15 Sep 1978; publ. 1979 (CONFIDENTIAL), pp. 49-73.

Fuller, K. N. G., Fox, P. G., and Field, J. E., "The Temperature Rise at the Tip of Fast-Moving Cracks in Glassy Polymers," Proceedings of the Royal Society of London, Ser. A, Vol. 341, No. 1627, 1975, pp. 537-557.

Hearle, J. W. S., Sparrow, J. T., and Cross, P. M., The Use of the Scanning Electron Microscope (Oxford: Pergamon Press, 1972).

Kendall, K., "Complexities of Compression Failure," Proceedings of the Royal Society of London, Ser. A, Vol. 361, No. 1705, 1978, pp. 245-263.

Kincaid, J. F., "The Inadvertent Detonation of Large Solid Motors Loaded with High Energy Propellants," in ONR/AFOSR Workshop on Deflagration-to-Detonation Transition, CPIA Publ. 299, 11-13 Jan 1978; publ 1978, pp. 5-18.

Knollman, G. C., Martinson, R. H., and Bellin, J. L., "Ultrasonic Assessment of Cumulative Internal Damage in Filled Polymers," Journal of Applied Physics, Vol. 50, No. 1, 1979, pp. 111-120.

Krautkramer, J. and Krautkramer, H., Ultrasonic Testing of Materials (New York: Springer-Verlag, 1969), pp. 151-196.

Lawn, B. R. and Wilshaw, T. R., Fracture of Brittle Solids (Cambridge: Cambridge University Press, 1975), pp. 5-9.

Liddiard, T. P., "The Initiation of Burning in High Explosives by Shock Waves," in Proceedings of the Fourth Symposium on Detonation, Publ. ACR-126, 12-15 Oct 1965; publ 1966, pp. 487-495.

Murri, W. J., Horie, Y., and Curran, D. R., "Fracture and Fragmentation of High Energy Propellant", SRI International Annual Report, Mar 1978.

Oberth, A. E., "Principle of Strength Reinforcement in Filler Rubbers," Rubber Chemistry and Technology, Vol. 40, No. 5, 1967, pp. 1337-1363.

Pollard, H. F., Sound Waves in Solids (London: Pion Ltd., 1977), pp. 157-159.

Richardson, J. H., Optical Microscopy for the Materials Sciences (New York: Marcel Dekker, Inc., 1971).

Shimizu, M. and Tanemura, T., "Fracture Energy of a Composite Solid Propellant," in Proceedings of the Mechanical Behavior of Materials Symposium, Vol. I, 21-24 Aug 1974; publ 1974, pp. 589-598.

Weichert, R. and Schönert, K., "Heat Generation at the Tip of a Moving Crack," Journal of the Mechanics and Physics of Solids, Vol. 26, No. 3, 1978, pp. 151-161.

Winter, R. E. and Field, J. E., "The Role of Localized Plastic Flow in the Impact Initiation of Explosives," Proceedings of the Royal Society of London, Ser. A, Vol. 343, No. 1634, 1975, pp. 399-413.

VI. ABBREVIATIONS, ACRONYMS, AND SYMBOLS

V_L	longitudinal sound velocity	m/s
e	engineering strain	%
l	final sample length	mm
l_o	initial sample length	mm
f_c	center frequency	MHz

APPENDIX A

MODEL OF THE FAILURE PROCESS IN COMPOSITE SOLID PROPELLANTS

Tensile failure in composite solid propellants is considered to occur in a multiple step process. Shimizu and Tanemura¹⁹ list the following sequence of events (except at very low temperatures):

- (1) Underwetting process - elastic deformation before the initiation of separation between the binder-filler interface.
- (2) Dewetting process - initiation and growth of vacuoles.
- (3) Tearing process - crack initiating and growing to be catastrophically large crack.
- (4) Rupture process - after the start of abrupt macro-rupture from one of the catastrophically large cracks.

Although the above is strictly for tensile failure, similar processes are envisioned for composite propellants subjected to compressive stresses.

¹⁹ Shimizu, M. and Tanemura, T., "Fracture Energy of a Composite Solid Propellant," in Proceedings of the Mechanical Behavior of Materials Symposium, Vol. I, 21-24 Aug 1974; publ 1974, pp. 589-598.

DISTRIBUTION

	<u>Copies</u>		<u>Copies</u>
Chief of Naval Material Washington, DC 20360	1	Office of Chief of Naval Operations Operations Evaluation Group (OP03EG) Washington, DC 20350	1
Commander Naval Air Systems Command Attn: Technical Library Department of the Navy Washington, DC 20361	1	Scientific and Technical Information Facility, NASA P. O. Box 33 College Park, MD 20740	1
Commander Naval Sea Systems Command Attn: SEA-09G32 Department of the Navy Washington, DC 20362	2	Commanding Officer Naval Weapons Station Attn: Technical Library Yorktown, VA 23691	1
Director Strategic Systems Project Office Attn: J. F. Kincaid E. L. Throckmorton, Jr.	1 1	Commanding Officer Naval Propellant Plant Attn: Technical Library Indian Head, MD 20640	1
Department of the Navy Washington, DC 20376		Superintendent Naval Academy Attn: Library Annapolis, MD 21402	1
Office of Naval Research Attn: ONR-741 (Technical Library) Department of the Navy Arlington, VA 22217	2	Naval Plant Representative Office Strategic Systems Project Office Lockheed Missiles and Space Company Attn: Technical Library P. O. Box 504 Sunnyvale, CA 94088	1
Commander Naval Weapons Center Attn: Technical Library R. L. Derr T. Boggs China Lake, CA 93555	1 1 1	Hercules Incorporated Allegany Ballistics Laboratory Attn: Technical Library K. Hartman P. O. Box 210 Cumberland, MD 21502	1 1
Director Naval Research Laboratory Attn: Technical Information Section Washington, DC 20375	1		

DISTRIBUTION (Cont'd)

<u>Copies</u>	<u>Copies</u>
Redstone Scientific Information Center	Director
U. S. Army Missile Command	Los Alamos Scientific Laboratory
Attn: Chief, Documents 1	Attn: Technical Library 1
Redstone Arsenal, AL 35809	B. G. Craig 1
	P. O. Box 1663
	Los Alamos, NM 87544
Commanding Officer	
Army Armament Research and Development Command	Aerojet Ordnance and Manufacturing Company
Attn: Technical Library 1	9236 East Hall Road
Dover, NJ 07801	Downey, CA 90241 1
Commanding General	
Attn: BRL 1	Hercules Incorporated Research Center
Aberdeen Proving Ground, MD 21005	Attn: Technical Information Division 1
	Wilmington, DE 19899
Commanding Officer	
Harry Diamond Laboratories	Thiokol/Huntsville Division
Attn: Technical Library 1	Attn: Technical Library 1
2800 Powder Mill Road	Huntsville, AL 35807
Adelphi, MD 20783	
Armament Development and Test Center	Stanford Research Institute
DLOSL/Technical Library	Attn: Technical Library 1
Eglin Air Force Base, FL 32542 1	D. Curran 1
	333 Ravenswood Avenue
	Menlo Park, CA 94025
Director	
Applied Physics Laboratory	Thiokol/Wasatch Division
Attn: Technical Library 1	Attn: Technical Library 1
Johns Hopkins Road	P. O. Box 524
Laurel, MD 20810	Brigham City, UT 84302
Director	
Defense Technical Information Center	Thiokol/Elkton Division
Cameron Station	Attn: Technical Library 1
Alexandria, VA 22314 12	P. O. Box 241
	Elkton, Md 21921
Lawrence Livermore Laboratory	
University of California	Rohm and Haas
Attn: Technical Library 1	Huntsville, Defense Contract Office
E. James 1	Attn: H. M. Shuey 1
E. L. Lee 1	723-A Arcadia Circle
P. O. Box 808	Huntsville, AL 35801
Livermore, CA 94550	

DISTRIBUTION (Cont'd)

Copies

Pennsylvania State University
Department of Mechanical
Engineering
Attn: K. Kuo
University Park, PA 16802 1

Hercules Incorporated,
Bacchus Works
Attn: Technical Library 1
B. Hopkins 1
J. Thacher 1
P. O. Box 98
Magna, UT 84044

Chemical Propulsion Information
Agency
The Johns Hopkins University
Applied Physics Laboratory
Johns Hopkins Road
Laurel, MD 20810 1

Brigham Young University
Department of Chemical Engineering
Attn: Dr. M. W. Beckstead 1
Provo, UT 84601

Lockheed Palo Alto Research
Laboratory
Attn: Technical Library 1
H. P. Marshall 1
R. H. Martinson 1
3251 Hanover Street
Palo Alto, CA 94304

Air Force Rocket Propulsion
Laboratory
Attn: Technical Library 1
R. L. Geisler 1
Edwards Air Force Base, CA 93523

National Bureau of Standards
Attn: G. V. Blessing 1
Sound Building, A147
Ultrasonic Standards
Washington, DC 20234

TO AID IN UPDATING THE DISTRIBUTION LIST
FOR NAVAL SURFACE WEAPONS CENTER, WHITE
OAK TECHNICAL REPORTS PLEASE COMPLETE THE
FORM BELOW:

TO ALL HOLDERS OF NSWC/TR 79-259
by Wayne L. Elban, Code R11

DO NOT RETURN THIS FORM IF ALL INFORMATION IS CURRENT

A. FACILITY NAME AND ADDRESS (OLD) (Show Zip Code)

NEW ADDRESS (Show Zip Code)

B. ATTENTION LINE ADDRESSES:

C.

☐ REMOVE THIS FACILITY FROM THE DISTRIBUTION LIST FOR TECHNICAL REPORTS ON THIS SUBJECT.

D. NUMBER OF COPIES DESIRED _____

DEPARTMENT OF THE NAVY
NAVAL SURFACE WEAPONS CENTER
WHITE OAK, SILVER SPRING, MD. 20910

OFFICIAL BUSINESS
PENALTY FOR PRIVATE USE, \$300

POSTAGE AND FEES PAID
DEPARTMENT OF THE NAVY
DOD 316



COMMANDER
NAVAL SURFACE WEAPONS CENTER
WHITE OAK, SILVER SPRING, MARYLAND 20910

ATTENTION: CODE R11

